VARIABILITY OF THE LATENT HEAT FLUX DURING 1988-2005

Shinsuke Iwasaki and Masahisa Kubota

School of Marine Science and Technology, Tokai University 3-20-1, Orido, Shimizu, Shizuoka, Shizuoka, JAPAN
E-mail: iwasaki@mercury.oi.u-tokai.ac.jp

ABSTRACT: Recently, several satellite data analyses projects and numerical weather prediction (NWP) reanalysis projects have produced the ocean surface Latent Heat Flux (LHF) data sets in the global coverage. Comparisons of these LHF data sets showed substantial discrepancies in the LHF values. Recently, the increase of LHF in during 1970s-1990s over the global ocean is shown by the LHF data that have been developed at the Objective Analyzed Air-Sea Fluxes (OAFlux) project. It is interesting to investigate the existence of the increase of LHF over a global ocean in the other LHF products. It is interesting to investigate the existence of the increase of LHF over a global ocean in the other LHF products. In this study, we assessed the consistencies and discrepancies of the inter-annual variability and decadal trend for the period 1988-2005 among six LHF products ((J-OFURO2, HOAPS3, IFREMER, NCEP1,2 and OAFlux) over the global ocean. As results, all LHF products showed a positive trend. In particular, the positive trend in satellite-based data analyses (J-OFURO2, HOAPS3, IFREMER) is larger than that in reanalysis products (NCEP1/2). Also, the consistencies and discrepancies are shown on the spatial patterns of the LHF trends across the six data sets. The positive trend of LHF is remarkable in the regions of western boundary currents such as the Kuroshio and the Gulf Stream in all LHF data sets. But, the discrepancies are shown on the spatial patterns of the LHF trends in tropics and subtropics. These discrepancies are primarily caused by the differences of the input meteorological state variables, particularly for the air specific humidity, used to calculate LHF.

KEY WORDS: Latent heat flux, Satellite data, Hydrological cycle, Evaporation.

1. INTRODUCTION

Ocean surface latent heat flux (LHF) is the process which exchange of water and heat at the air-sea interface. Therefore, the LHF is necessary in understanding the hydrological cycle, the surface heat budget and the upper ocean salinity budget. The LHF has been primarily estimated from the bulk algorithms as functions of the wind speed at the 10m (U10), the sea surface specific humidity (Qs) and then air specific humidity (Qa) such that

$$LHF = \rho \; Lv \; Ce \; U10 \; (Qs-Qa). \qquad (1)$$

Where ρ is the density of air; Lv is the latent heat of vaporization; Ce is a bulk coefficient and is determined by the atmospheric stability, the air-sea temperature differences, and wind speed.

The satellite observations can provide the necessary parameters (U10, Qs and Qa) for estimating the LHF with global ocean coverage. Currently, there are several datasets of global ocean LHF, which are based on the U10 and the Qa derived from the microwave sensors such as the Special sensor Microwave Imager (SSM/I) on board a series of the Defence Meteorological Satellite Program (DMSP) spacecraft. In addition, various re-analysis products of the data assimilation systems with atmospheric general circulation models (GCM) can provide global ocean LHF. Comparisons of these LHF data sets showed substantial discrepancies in the LHF value (Kubota et al., 2003).

Recently, the increase of LHF in during 1970s-199s over the global ocean is shown by the LHF data that have been developed at the Objective Analyzed Air-Sea Fluxes (OAFlux) project (Yu, 2007). Tomita and Kubota (2005) also showed increase in turbulent heat flux during the 1990s over the Kuroshio/Oyashio extension region. Recently, several satellite data analyses and re-analysis projects have produced new versions of the LHF data sets. It is interesting to investigate the existence of the increase of LHF over global ocean in the other LHF products.

In this study, we assessed the consistencies and discrepancies of the inter-annual variability and decadal trend for the period 1988-2005 among the ocean surface LHF from recent satellite-based data sets and re-analysis products over the global ocean.

2. GLOBAL LHF DATA

We used six different data sets of the LHF, including three satellite-based data sets, two reanalysis products and one data that combined satellite data and reanasis data and in-situ data (ship and buoy). Basic descriptions of the global LHF data sets are provided in Table 1. The three satellite-based data sets are the Japanese Ocean Flux data sets with Use of Remote sensing Observation Version 2 (J-OFURO2), the Hamburg Ocean-Atmosphere Parameters and Fluxes Version 3 (HOAPS3) and the IFREMER. The two reanalysis products are NCEP/NCAR Reanalysis (NRA1) and NCEP/DOE

AMIP2 Reanalysis (NRA2). The other data is the Objectively Analyzed Air-Sea Fluxes (OAFlux). The time period selected for this study is 1988-2005. But, the data during 1993-2005 for IFREMER since the time period of this data is from March 1992. The temporal resolutions of all the LHF data sets are based on yearly mean value. Also, the spatial resolutions of these are converted to 1° grid sizes. Moreover, We also used the necessary parameter (U10, Qs and Qa) for estimating the LHF. However, we not use these parameters for OAFlux because of there isn't that. It is 10m heights that Qa of the satellite-based data sets. At the same time, the heights are 2m Qa for reanalysis data sets. Therefore, the Qa for reanalysis are corrected to 10m using Fairall et al.,(2003) algorithm.

Table 1. Basic descriptions of the global LHF data sets.

	Time period	Spatial resolution	Reference
J-OFURO2	Jan 1988-Dec 2005	1°	Kubota and Tomita (2007)
HOAPS3	Jul 1987 – Dec 2005	0.5°	Andersson et al. (2007)
IFREMER	Mar 1992 – Dec 2007	1°	Unpublished
NRA1	Jan 1948 - present	T62 Gaussian	Kalnay et al.(1996)
NRA2	Jan 1979 – present	T62 Gaussian	Kanamitsu et al.(2002)
OAFlux	Jan 1958 – Dec 2006	1°	Yu (2007)

3. RESULTS

Figure 1 shows the anomaly time series of the yearly averaged LHF over the 60°S-60°N. In general, all data sets show a systematic increase in LHF the 18 years. The J-OFURO2 and the IFREMER are the large negative anomaly during 1992-1995. The other side, the J-OFURO2 and IFREMER are the large positive anomaly during 2000-2005. The HOAPS3 is a large negative anomaly in the 1991. Table 2 also shows the trends calculated from yearly averaged LHF. In Table 2 the trends for the satellite-based data sets (J-OFURO2, HOAPS3) are larger compared with these of other data. In addition, the trend for OAFlux is the smallest.

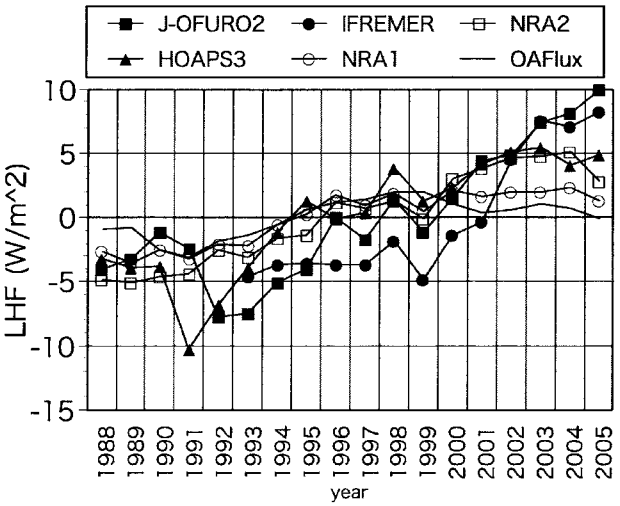

Figure 1. Anomaly time series of the yearly averaged LHF(W/m^2) over the region 60°S-60°N.

Table 2. Trends of the LHF over the region 60°S-60°N.

J-OFURO2	HOAPS3	NRA1	NRA2	OAFlux
14.12	12.44	6.02	10.84	3.12

Unit in (W/m^2/18year)

To understand the discrepancies among the time series for the different LHF data sets, we examine the variations of the input parameter in the bulk algorithms. Figure 2 shows the anomaly time series of the yearly averaged U10, specific humidity differences (DQ), Qs and Qa over the region 60°S-60°N. From Figure 2, it is clear that the U10 and the DQ for all data increase the period from 1988-2005. Also, the increase of the DQ influences an increase of the Qs. For U10, the J-OFURO2 shows a tendency greatly different from other data. This is a tendency due to use many kinds of satellite data (Kubota and Tomita 2007). In the time series of DQ, the trends for the satellite-based data set are larger than these other data. The time series of Qs clearly show tendency difference for all data is small. However, HOAPS3 shows an extreme cold SST in 1991, which leads to a spike in the HOAPS3 LHF. The timing of this spike suggests an inappropriate retrieval of SST in response to the eruption of Mount Pinatubo (Klepp et al., 2008). The other side, the Qa shows large difference in each of data sets. The Qa for J-OFURO2 and IFREMER show negative anomaly during 2001-2005. However, the Qa for other data sets shows positive anomaly.

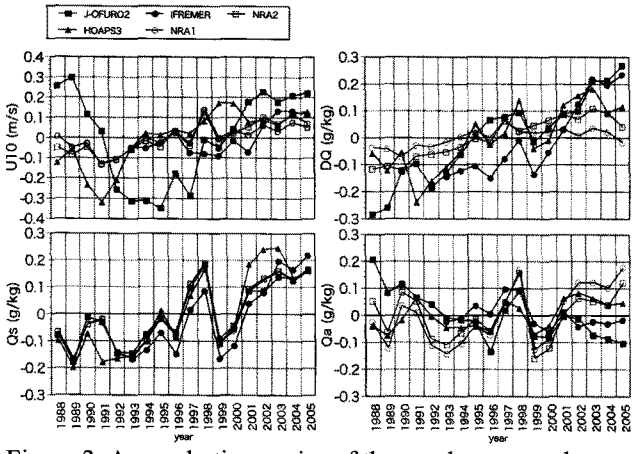

Figure 2. Anomaly time series of the yearly averaged input parameters (U10, DQ, Qs, Qa) over the region 60°S-60°N.

Figure 3 also shows the trends for the Trends of Input parameters (U10, DQ, Qs, Qa) for the period 1988-2005. From the Figure 3, the all input parameter for most data sets show positive trends. But, the Qa for J-OUFOR2 is only negative trend. As result, the DQ for J-OFURO2 is largest trend. Also, the trend of U10 and Qs for HOAPS3 is larger compared with other data sets. This is due to large negative anomaly for U10 and Qs in 1991.

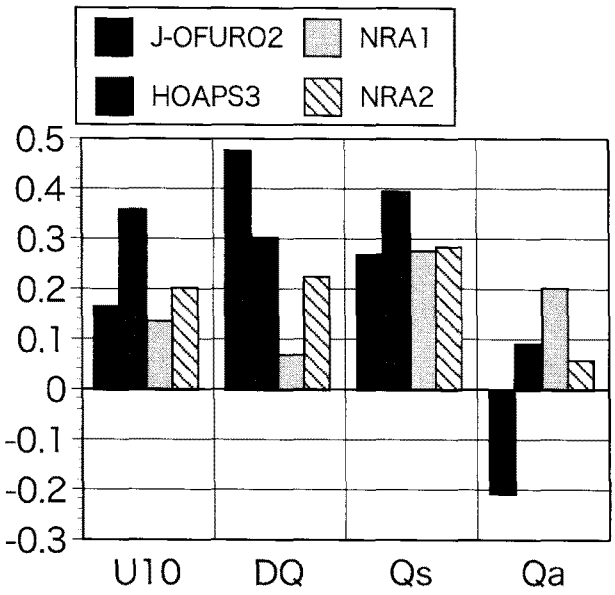

Figure 3. Trends of Input parameters (U10, DQ, Qs, Qa) over the region 60°S-60°N.

Figure 4 shows the spatial distributions of the LHF trends. The all data sets of LHF show increasing trends over the western boundary current regions of the Kuroshio and Gulf Stream. The increase for LHF over the Kuroshio is a consistent with results of Tomita and Kubota (2005). Also, the satellite-based two data sets (J-OFURO2, HOAPS3) are similar distributions. The discrepancies of between satellite-based data sets and other data sets are shown on the spatial patterns of the LHF trends in tropics and subtropics.

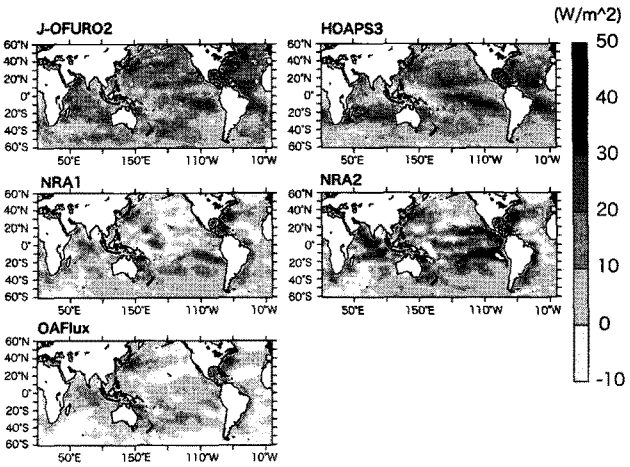

Figure 4. Spatial distributions of the LHF trends (W/m^2/18 year) over the period 1988-2005.

The increased of ocean surface LHF is closely related to atmospheric water vapor. Recent satellite observations of the column-integrated water vapor (precipitable water) from SSM/I that atmospheric moisture amounts have been rising since the beginning of the data record in 1988 (Trenberth et al., 2005; Yu, 2007). Figure 5 shows anomaly time series of the yearly averaged evaporation from the J-OFURO2 LHF and the column-integrated water vapor over the global ocean from SSM/I. It is clear that the upward tendencies of the two curves have good consistency. Also, Table 3 shows temporal correlation coefficients between the yearly averaged evaporation from the J-OFURO2 LHF and the yearly averaged column-integrated water vapor over the global ocean from SSM/I. From this result, the correlation coefficient for J-OFURO2 is highest. On the other hand, the correlation coefficient for OAFlux is lowest.

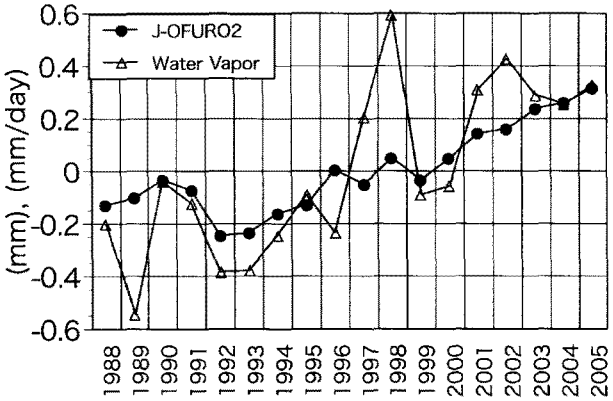

Figure 5. Anomaly time series of the yearly averaged evaporation from the J-OFURO2 LHF and the column-integrated water vapor over the global ocean from SSM/I.

Table 3. Temporal correlation coefficients between the yearly averaged evaporation from the J-OFURO2 LHF and the yearly averaged column-integrated water vapor over the global ocean from SSM/I.

J-OFURO2	HOAPS3	NRA1	NRA2	OAFlux
0.78	0.75	0.75	0.75	0.52

4. CONCLUSION

We assessed the consistencies and discrepancies of the inter-annual variability and decadal trend for the period 1988-2005 among six LHF products. As results, all LHF products showed a positive trend. The increase in the U10 and Qs has the large contribution to the increase n LHF. In particular, the positive trend in satellite-based data analyses (J-OFURO2, HOAPS3, IFREMER) has larger than that in reanalysis products (NCEP1/2). Also, from the spatial distributions of the LHF trends shows increasing trends over the western boundary current regions of the Kuroshio and Gulf Stream. But, the discrepancies of between satellite-based data sets and other data sets are shown on the spatial patterns of the LHF trends in tropics and subtropics. Moreover, we has confirmed not only an increase in the LHF but also an increase column-integrated water vapor.

ACKOWLEDGMENT:

This study was supported by the Japan Aerospace Exploration Agency (JAXA).

REFERENCE

Andersson, A., S. Bakan, and C. Klepp, 2007. The HOAPS Climatology. *FLUX NEWS* , 4, 10-12

Klepp, C., A. Andersson, and S. Bakan, 2008. The HOAPS Climatology: Evaluation of Latent Heat Flux. *FLUX NEWS*, 5, 30-32.

Fairall, C. W., J. E. Hare, A. A. Grachev, and J. B. Edson, 2003. Bulk parameterization of air-sea fluxes. *J. Climate,* 16, 571-591.

Kalnay, E., and Coauthors, 1996. The NCEP/NCAR 40-Year Reanalysis Project. *Bull. Amer. Meteor. Soc.,* 77, 437-471.

Kanamitsu, M., W. Ebisuzaki, J. Woollen, S. K. Yang, J. J. Hnilo, M. Fiorino, and G. L. Potter, 2002. NCEP/DOE AMIP-2 reanalysis (R-2). *Bull. Amer. Meteor. Soc.,* 83, 1,631-1,643.

Kubota, M., A. Kan, H. Muramatsu, and H. Tomita, 2003. Intercomparison of various surface latent heat flux fields. *J. Climate,* 16, 670-678.

Kubota, M., and H. Tomita, 2007. The Present State of the J-OFURO Air-Sea Interaction Data Product. *FLUX NEWS*, 4, 13-15.

Liu, J., and J. Curry, 2006. Variability of the tropical and subtropical ocean surface latent heat flux during 1989-2000. *Geophys. Res. Lett.,* 33, L05706, doi:10.1029/2005GL024809.

Tomita, H., and M. Kubota, 2005. Increase in turbulent heat flux during the 1990s over the Kuroshio/Oyashio extension region, *Geophys. Res. Lett.,* 32, L09705, doi:10.1029/2004GL022075.

Trenberth, K. E., J. Fasullo, and L. Smith, 2005. Trends and variability in column-integrated atmosperic water vapor. *Climate Dyn.,* 24, 741-758.

Yu, L., and R. A. Weller, 2007. Objectively Analyzed Air-Sea Heat Fluxes for the Global Ice-Free Oceans (1981-2005). *Bull. Amer. Meteor. Soc.,* 88, 527-539.